Journal of Non-Crystalline Solids 560 (2021) 120732

Contents lists available at ScienceDirect

Journal of Non-Crystalline Solids

journal homepage: www.elsevier.com/locate/jnoncrysol

# The effect of Ag substitution on physico-chemical and biological properties of sol-gel derived 60%$SiO_2$-31%CaO-4%$P_2O_5$-5%$TiO_2$ (mol%) quaternary bioactive glass

Amirhossein Moghanian [a,*], Saba Nasiripour [a], Seyed Mohammad Hosseini [b], Seyed Hesamedin Hosseini [a], Ali Rashvand [a], Alireza Ghorbanoghli [c], Arang Pazhouheshgar [d], Fariborz Sharifian Jazi [e]

[a] Department of Materials Engineering, Imam Khomeini International University, Qazvin 34149-16818, Iran
[b] Qazvin Science and Technology Park, Qazvin 34719-91984, Iran
[c] Department of Materials Science and Engineering, K. N. Toosi University of Technology, Tehran 19395-1999, Iran
[d] School of Mechanical Engineering, Iran University of Science and Technology, Tehran 16846-13114, Iran
[e] Mining and Metallurgical Engineering Department, Amirkabir University of Technology, Tehran 15875-4413, Iran

ARTICLE INFO

*Keywords:*
Hydroxyapatite
*In vitro* bioactivity
Sol-gel processes
$TiO_2$
$Ag_2O$

ABSTRACT

This research presents an investigation on the simultaneous effect of titanium (Ti) and silver (Ag) on structural and biological behaviors of the co-substituted 58S bioactive glass. Structural and morphological characterizations were studied by means of X-ray diffraction (XRD) analysis, Fourier transform infrared spectrum (FTIR), scanning electron microscopy (SEM) as well as Energy-dispersive X-ray Spectroscopy (EDS) analysis. The structural results exhibited that the hydroxyapatite)HA) layer was formed on the T/A-BGs after the 7th day of immersion in simulated body fluid)SBF(solution and increased overtime. Furthermore, the trend of cell proliferation and antibacterial activity were the same and by increasing Ag percentage up to 8 mol.% firstly, mentioned properties increased and then decreased. Hence, T/A-BG containing fixed 5 mol.% Ti and 2 mol. % Ag (TA2 (indicated higher *in vitro* biological performance compared to other synthesized T/A-BGs and suggested as an optimal specimen for further clinical applications.

## 1. Introduction

Tissue engineering (TE) is an interesting, complex, dynamic, and effective approach to solve the problems of bone defects. It has been used in different medical extents such as traumatology, orthopedics, oncology, and dentistry. The main purposes of TE are to repair, replace, or enhance the function of biological substitutes [1]. Additionally, the emergence of TE has been responded to many diseases [2]. Moreover, the synthesis and design of new biomaterial can be a response to requirements [3]. Furthermore, bioactive glass(BG) emerged as an effective biomaterial to play important roles in different fields, especially in medical.

BG in the system of CaO − $P_2O_5$ and $SiO_2$ is one of the promising biomaterials for bone regeneration and can bond to bone [3–5]. The biomaterials with the ability of hydroxyapatite (HA) formation on their surface are bioactive [6,7]. Meanwhile, bioactivity plays a significant role in biomaterials function [8]. The first synthesized BG, 45S5, was invented by professor Hench [9] and was developed by different modified chemical compositions such as 58S [10], 68S [11,12], and 77S [13]. The main reasons for various BGs applications are due to their properties such as bioactivity [14,15], osteogenesis [16], controllable biodegradability [17], as well as antibacterial efficiency [18,19].

There are various fabrication methods for synthesizing of BGs that have been reported, such as conventional melt quench, flame synthesis, and microwave irradiation, as well as sol-gel [20]. The preferences of sol-gel in comparison with other methods are its speed and easiness. Additionally, it can be controlled to be achieved required products with a high degree of purity and homogeneity and it makes an extensive range of composition synthesis [20,21]. In recent years, the applications of BGs have been become extent because of their positive effect in different fields such as: dental and bone implants [22,23], load-bearing scaffold due to their strength and good mechanical properties [24–26] as

* Corresponding author.
*E-mail address:* Moghanian@eng.ikiu.ac.ir (A. Moghanian).

https://doi.org/10.1016/j.jnoncrysol.2021.120732
Received 1 December 2020; Received in revised form 30 January 2021; Accepted 10 February 2021

well as the design of light-triggered and targeted drug delivery hybrids [27,28]. Till now, many modified BGs have been investigated by individual addition of various amount elements such as: magnesium (Mg) [29], strontium (Sr) [30], copper (Cu) [31], zinc (Zn) [32], lithium (Li) [33], titanium (Ti) [34] and silver (Ag) [35] in bone tissue engineering (BTE) applications.

Titanium (Ti) is a chemical element with an atomic number 22 and an atomic mass is 47.867 $g.mol^{-1}$ [36]. Besides, the oxidization of Ti affected antibacterial activity of Ti- substituted BG (Ti-BG) and improved it [37]. The antibacterial properties of BG have been previously noted [38]. Furthermore, silver is an element with the atomic symbol: Ag, atomic number: 47, and atomic weight of 107.8682 $g.mol^{-1}$ [39]. Moreover, it is used in both ionic and metallic forms [40]. Silver nitrate is an inorganic Ag compound that improves the *in vitro* bioactivity and antibacterial efficiency [41,42]. On the other hand, the bacteria can endanger the human body and BG can be a positive response to them [11]. Moreover, BG containing Ag and Ti plays a more influential role against bacteria [43]. Methicillin-resistant staphylococcus aureus (MRSA) bacteria is the major type of staphylococcus aureus infection that shows resistance against antibiotics [44]. Therefore, the antibacterial activity of BGs has usually been investigated against MRSA [45,46].

Till now, several studies have focused on the effect of Ag on *in vitro* biological behavior, bioactivity, and bactericidal activity of sol-gel derived BGs and then reported the various optimum element's content in BG's composition to be achieved the highest desirable properties [2,33]. On the one hand, some researchers agreed with the positive effect of Ag on cell proliferation and cell viability in mechanical alloying (MA) and powder metallurgy (PM) derived Ti/Ag-substituted 45S5 BGs [43,47]. Moreover, the addition of Ag in the range of 1-3 mol.% was reported as an optimum percentage, while others had reverse investigations on the optimum amount of Ag in Ag-substituted BGs for use in clinical applications [15]. Furthermore, in previous studies 5 mol. % Ti was announced as an optimum amount in Ti-substituted BGs (T-BG). As far as we searched, the consideration of the simultaneous effect of Ag and Ti in the silicon-based BG was not extensive and was limited to small amounts of Ag [43,47]. Thus, it was decided to investigate the effect of various amounts of Ag on the biological and structural behavior of T/ABGs. Our goal was to consider how different Ag amounts affect *in vitro* bioactivity and bactericidal efficiency as two major factors in clinical applications such as drug delivery and *in vivo* evaluation in rat and rabbit models after as a novel multifunctional bioactive material with enhanced *in vitro* bioactivity, cell proliferation and antibacterial [48,49]. This study followed the effect of substituting up to 8 mol. % of $Ag_2O$ for CaO on *in vitro* bioactivity, biocompatibility, alkaline phosphatase (ALP), and antibacterial activity of sol-gel derived 58S BGs with formula 60 % $SiO_2$-(31-x) % CaO-4 % $P_2O_5$-5 % $TiO_2$-X % $Ag_2O$ which (X=0, 1, 2, 4, 6, and 8 mol. %) as a major aim. In other words, in this research the various amount of Ag was utilized to be investigated the changes of the morphology and the structure of synthesized T/A-BGs due to *in vitro* formation of HA on their surfaces by X-ray diffraction (XRD) analysis, fourier transform infrared spectrum (FTIR), scanning electron microscopy (SEM) as well as energy dispersive X-ray spectrometry (EDS). Besides, investigation the effect of Ag on cell proliferation, cell viability, and bactericidal efficiency of synthesized T/A-BG was studied by (ALP) activity, 3- (4, 5dimethylthiazol-2-yl)-2, 5-diphenyltetrazolium bromide (MTT) assay as well as antibacterial activity against MRSA bacteria respectively, due to investigation of the optimum amount of $Ag_2O$ in novel sol-gel derived synthesized T/A-BG.

## 2. Material and methods

### 2.1. Materials

The T/A-BGs were synthesized by sol-gel method in the system of 60 % $SiO_2$-(31-X) % CaO-4% $P_2O_5$ 5% $TiO_2$-X% $Ag_2O$ (which X = 0, 1, 2, 4, 6, and 8 mol. %). Tetraethyl orthosilicate ($Si(OC_2H_5)_4$ -TEOS, Merck), triethyl phosphate ($(C_2H_5)_3PO_4$ -TEP, Merck), calcium nitrate tetrahydrate ($Ca(NO_3)_2.4H_2O$, Merck), Tetraethyl orthotitanate ($C_2H_5O)_4Ti$-(TEOT), Sigma-Aldrich, St Louis, Mo) and Ag nitrate with the formula ($AgNO_3$, Sigma-Aldrich). Meanwhile, for evaluating *in vitro* biological properties of T/A-BGs, SBF solution was used. Nitric acid and deionized water were also used to provide a dissolution basis. After synthesizing the T/A BGs powders, 9 MPa pressure was applied to powders to be achieved discs with 1cm diameter and 0.3 g weight by a hydraulic press. Afterward, for *in vitro* evaluations, discs were soaked in 15 ml SBF solution, which was prepared according to Kokubo's protocol [50], for 7 and 14 days and then removed from the SBF solution.

### 2.2. BGs synthesis

The synthesis of sol-gel derived T/A-BGs with a fixed amount of 5 mol. % and different concentrations of Ag (0, 1, 2, 4, 6, and 8) mol. % began by stirring the mixture of 0.1 N nitric acid solution and TEOS by a magnetic stirrer for about 30 min. In the following, TEP and calcium nitrate tetrahydrate were added and stirred, and in the last steps for preparation of sol, Ti and Ag were added in 2 distinct stages, respectively. At all stages, the mixing time continued until the transparent sol was obtained. The mixture of the precursor was done without any additional heat at room temperature. Afterward, 7 days of natural aging of the finalized sol were performed by keeping in the container, enclosed with a perforated foil, in a place without any movement at 25 °C. In the following, the container was kept 3 days in the oven at 80°C to complete the water evaporation and for removal of residual nitrates and condensation of silanol groups, the obtained powders were calcined in the furnace at 700°C for 3h. then, grounded and as the final stage of preparation, shaped as disc-shaped specimens. All compositions of synthesized T/A-BGs are exhibited in Table 1

Meanwhile, due to the high compositional similarity of simulated body fluid (SBF) solution to human blood plasma, Biological assessments were performed by immersion of specimens in the SBF solution.

### 2.3. Characterization of synthesized T/A-BGs

#### 2.3.1. Thermal analysis

To study the thermal behavior of TA specimens, the TA specimen with the maximum amount of Ag was characterized by different thermal analysis (DTA) and thermogravimetric analysis (TGA), and finally, stabilizing temperature was detected. The DTA/TGA test was carried out by Shimadzu DSC-50 apparatus under an $N_2$ atmosphere (50 ml/min) in the temperature range of (25-1100)°C with the constant heating rate of 10°C/min.

#### 2.3.2. X-ray diffraction analysis

To examine the formation of HA on BGs surfaces, the T/A BGs specimen's surfaces were subjected to X-ray diffraction, after immersion in SBF solution for 7 and 14 days with X-ray source (Cu-Kα radiation) at 40 kV and in a 2θ range of 20° – 40°.

#### 2.3.3. Scanning electron microscopy (SEM) and energy-dispersive X-ray spectroscopy (EDS)

After immersion in SBF solution, scanning electron microscopy

**Table 1**
All compositions of synthesized T/A BGs in mol.%

| Bioactive glass | Lable | $SiO_2$ | CaO | $P_2O_5$ | $TiO_2$ | $Ag_2O$ |
|---|---|---|---|---|---|---|
| 58S-5%$TiO_2$-0%$Ag_2O$ | TA0 | 60 | 31 | 4 | 5 | 0 |
| 58S-5%TiO2-1%$Ag_2O$ | TA1 | 60 | 30 | 4 | 5 | 1 |
| 58S-5%TiO2-2%$Ag_2O$ | TA2 | 60 | 29 | 4 | 5 | 2 |
| 58S-5%TiO2-4%$Ag_2O$ | TA4 | 60 | 27 | 4 | 5 | 4 |
| 58S-5%TiO2-6%$Ag_2O$ | TA6 | 60 | 25 | 4 | 5 | 6 |
| 58S-5%TiO2-8%$Ag_2O$ | TA8 | 60 | 23 | 4 | 5 | 8 |

(SEM, MIRA3 TESCAN, Czech) was utilized to detect the surface morphology of the BG disks to appraise the formation and growth of HA over immersion time in SBF solution. Additionally, for analysis of formed HA on BG surface, the EDS test was done by (MIRA3 TESCAN, Czech) apparatus to be detected the elements and amount of elements.

#### 2.3.4. Fourier transform infrared spectroscopy (FTIR) analysis

FTIR spectroscopy (Nicolet, NEXUS 670) was used to investigate the formation of HA phase on the surfaces of the specimens before and after soaking in SBF solution by analyzing the change of functional groups by the 8 $cm^{-1}$ resolution and 400-4000 $cm^{-1}$ wavelength.

#### 2.3.5. Inductively coupled plasma-atomic emission spectroscopy (ICP-AES) and pH monitoring

Specimens kept in SBF solution were removed after 1, 3, 7, and 14 days and solutions for determining of Ca, Si, P, Ti, and Ag ions amount were analyzed by ICP-AES. Additionally, the diversity of pH in SBF solution was measured over time by a pH meter (Corning pH meter 340, USA) at each step.

### 2.4. Biological evaluation

#### 2.4.1. Live/dead assay

To determine the cell viability of T/A-BG specimens firstly, MC3T3-E1 cells were seeded at a density of 15000 cells/$cm^2$ on TA0 and TA2 and the media altered every other day up to 14 days. After the end of this trend in the period time, the cell culture was removed, and seeded cells were washed with phosphate buffered saline (PBS). Followed by, for preparing live/dead solution, 200 μL of 2 μM calcein-acetoxymethyl ester (calcein-AM, Sigma, USA) and 4 μM ethidium homodimer-1 (EthD-1, Sigma, USA) were incubated at 37°C in a humidified atmosphere of 5% $CO_2$ for 15 min in dark. Finally, PBS was chosen for cells-washing, and stained cells (live cells: green stained, dead cells: red stained) were observed under a fluorescence microscope (Olympus, USA) and concerned images were taken by the camera. Additionally, the green and red fluorescence were made by calcein-acetoxymethyl ester and ethidium homodimer-1, respectively. Besides, producing green cells was because of intracellular esterases in live cells and penetrating cells with damaged membranes and binding to nucleic acids led to producing red fluorescence in dead cells.

#### 2.4.2. MTT and ALP activity assays

To study the simultaneous effect of Ti and Ag on the biocompatibility of T/A-BGs, the 3- [4, 5-dimethylthiazol-2yl]-2, 5-diphenyl-2H tetrazolium bromide (MTT) assay was used to assess the proliferation of the MC3T3-E1 after in contact with T/A-BGs powders. MTT assay was based on the reduction of tetrazolium salt to formazan crystals by living cells. In this study, measuring the ALP enzyme investigated the osteoblastic activity of the MC3T3-E1 cells. Based on the manufacturer's recommendations (BioCat, Heidelberg, Germany), MC3T3-E1 cells were accounted at a density of $1 \times 10^4$ cells/$cm^2$ and plated and cultured in 24-well plates on specimens in a humidified atmosphere of 95% air and 5% carbon dioxide at 37°C for 7 and 14 days, and enzyme activity was determined at 410 nm for the amount of p-nitrophenyl liberated [33,51,52].

#### 2.4.3. Antibacterial studies

MRSA was diluted approximately from $0.5 \times 10^8$ to $2 \times 10^8$ $ml^{-1}$ [38,53] and was cultured in liquid lysogeny broth (LB) medium at 37°C to investigate the effect of Ag on antibacterial activities in Ti-substituted BGs. 0.9 ml LB medium was added into three 1.5 ml Eppendorf tubes containing 10 mg TA0 (control specimen), TA1, TA2, TA4, TA6, and TA8 particles, followed by stirring for 1 min. Then 0.1 ml bacterial suspension was added into each Eppendorf tube and the solutions were cultured at 37°C for 1 hour. After a serial dilution, 100 μl suspensions were plated onto LB-agar plates and immersed during the night at 37°C in the dark [38]. Meanwhile, the bactericidal efficiency was computed by counting the final colony-forming units per milliliter (CFU/mL) as follows [38,54,55].

$$\text{Bactericidal fraction} = 1 - (\text{number of survived bacteria} / \text{number of total bacteria})$$

## 3. Result and discussion

### 3.1. Thermal analysis

Based on the simultaneous thermal analysis (STA) that is exhibited in Fig. 1, the DTA/TGA analysis was carried out on the TA8 (specimen with maximum Ag amount) to determine the proper temperatures of different mass loss stages with a heating rate of 10°C/min. TGA result illustrated 4 special peaks i.e., the first weight loss (17%) from 50-150°C was ascribed to the release of water and alcohol [56]. The second weight loss (26%) commenced from 410-500°C, most likely due to the loss of the alkoxy group [57]. The third drop in mass occurred from 670°C to around 750°C with 15% weight loss which was associated with the removal of the residual nitrates as metal nitrate in the synthesis of the sol. The final peak (fourth), occurred around 1000°c that corresponded to the crystallization of CaSiO3 (β-wollastonite) and cristobalite [56]. Additionally, according to previous studies, it was stated that the substitution of 5 and 10 mol. % $TiO_2$ with CaO in sol-gel derived 45S5 BG led to an increase in the transition and crystallization temperatures because of ion radius of Ti (56 pm) is lower than the ion radius of Ca (100 pm) [58]. Besides, it was reported that sol-gel derived 58S-BG containing different percentages of substituted Ag exhibited a decrease in transition and crystallization temperatures that corresponded to ions radius of Ag (156pm) that in comparison to Ca with ion radius of (100 pm) [59]. Hence, in sol-gel derived 58S BG with fixed 5 mol.% Ti and 8 mol. % Ag, the Ti and Ag had the opposite effect on transition and crystallization temperatures in STA. Due to the ion radius of Ag was more than CaO it caused disruption in T/A-BG network and diminished the effect of Ti substituted in transition temperatures and decreased them. Taken together, 750°C was selected as the stabilization temperature for T/A-BG.

### 3.2. X-ray diffraction analysis

Fig. 2(a–c) illustrates XRD patterns of TA0, TA1, TA2, TA4, TA6, and TA8 before and after immersion in SBF solution for 7 and 14 days. As it was evident by increasing immersion time up to 14 days, the formed HA on T/A-BG surfaces increased. Additionally, the trend of formation of HA on the T/A-BG surface was completely different by the trend of increasing Ag percentage from 0 to 8 mol.% in T/A-BGs composition.

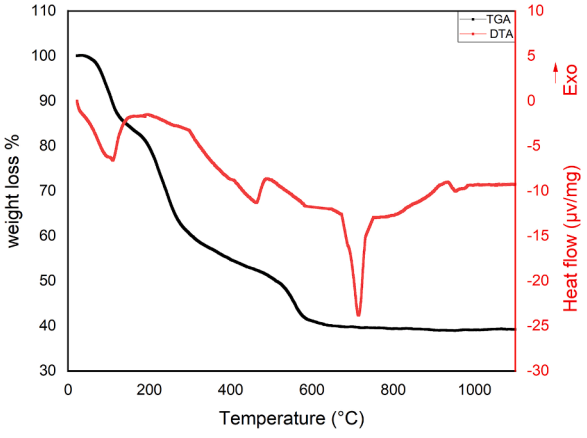


**Fig. 1.** The DTA/TGA curves of TA8.

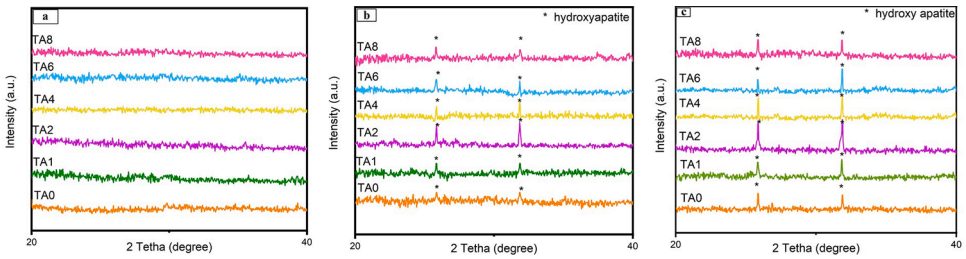


**Fig. 2.** XRD patterns of T/A-BGs before immersion (a) and after immersion in the SBF solution for 7 days (b) and 14 days (c).

According to Fig. 2(a), no peaks that corresponded to formed crystalline HA were found while, in Fig. 2(b) and (c) that were attributed to the immersion of specimens after 7 and 14 days, obviously HA peaks were detected [60]. Furthermore, the peaks intensity altered. In other words, the intensities of the peaks were changed by increasing the Ag percentages from 0 mol.% to 8 mol.%, the intensities of peaks firstly increased and then decreased. Although, the increasing immersion time had a positive effect on peaks intensities and led to an increase in them. Previously, Sharifianjazi et al. confirmed that by increasing Ag amount (2, 4, and 6 mol. %) in Ag-substituted 58S BG, the peaks intensity enhanced. Furthermore, by increasing immersion time up to 14 days, the amount of HA formed increased on the BG surface [56]. Additionally, Jurczyk et al. reported that in 45S5 BG substituted with 10 Ti and 1.5 Ag (mol. %), the first peaks of XRD patterns that corresponded to HA formation appeared after 15 h immersion in SBF solution [43]. Moreover, it was reported that 45S5 BG substituted with 10 Ti and 1 Ag (mol. %) showed the first peaks of P-O and C-O that related to HA formed after 15 h immersion in SBF solution. Hence, the T/A-BG by 5 Ti and 2 Ag (mol. %) (TA2) exhibited the highest bioactivity and maximum amount of HA formed on its surface in comparison to other specimens.

### 3.3. FTIR

Fig. 3(a–c) shows the FTIR spectroscopy of TA0, TA1, TA2, TA4, TA6, and TA8 in the spectral range of 4000-400 $cm^{-1}$ before and after soaking in the SBF solution for 7 and 14 days. These correspond to the peaks near 470, 1000-1100, and 1250 $cm^{-1}$ for the bending vibration of Si–O–Si [61,62], peak at 790 $cm^{-1}$ for the symmetric stretching of Si–O [63], as well as peaks at 1651 and 3500 $cm^{-1}$ for the stretching mode of the OH respectively [64]. Additionally, the bands located at (570,603) and (870,1455) $cm^{-1}$ were for the asymmetric bending mode of P-O and C-O groups, respectively [65,66] that proved the formation of HA layers after immersion for 7 and 14 days [67]. According to images, Fig. 3(a) showed no crystalline HA, Whiles, Fig. 3(b) and (c) exhibited the phosphate and carbonate peaks, and they were more significant on the 14th day of immersion. In addition, the intensity of peaks changed by increasing Ag percentage in Ag-substituted 58S BG. As it was obvious, these peaks were weak for the higher amount of Ti/Ag-BG, whiles they were more powerful for the lower percentage of Ti/Ag-BGs. Additionally, the highest intensity was seen in TA2. Besides, Buriti et al. [68] reported that sol-gel derived Ag-substituted 45S5 BG surface was a favorable substrate for apatite nucleation and deposition due to the presence of distinct phosphate bands in the FTIR spectrum. The FTIR results in Sharifianjazi. et al. study [56] proved that the time of HA formation in 58S-BG substituted with 2 mol. % Ag is earlier than sol-gel derived Ag-substituted 58S BG with 0 mol. % due to the FTIR spectrum of BG with 2 mol. % Ag appeared in 3 days after soaking but for free Ag BG it prolonged.

### 3.4. Surface morphology

The SEM images present the T/A-BGs surfaces before and after soaking in SBF solution. According to Fig. 4, the SEM images of TA0, TA1, TA2, TA4, TA6, and TA8 are exhibited after 7 and 14 days of immersion in SBF solution. Meanwhile, EDS analysis of formed HA on the surface of TA2 after immersion for 14 days in SBF solution is shown in Fig. 5. As it was evident, the HA globules were formed on the BG surface after 7 days of immersion, and it was considerable on the 14th day of immersion. Additionally, the amount of HA formed changed by increasing Ag percentage. As it was obvious, by increasing the Ag percentage, the HA amount firstly increased until 2 mol. %, and then it decreased up to 8 mol. %. In addition, according to Fig. 5, the EDS analysis exhibited the peaks of Si, P, Ca, C, O, Ti, and Ag and their intensities. Therefore, according to SEM and EDS analysis, it can be stated that the TA2 specimen exhibited the highest bioactivity in all T/A-BGs. According to the previous researcher, Jurczyk et al. [43] confirmed that Ti/Ag-incorporated BG could enhance bioactivity by increasing HA formed on its surface. Additionally, Sharifianjazi. et al. [56] affirmed that Ag-substituted 58S BGs with 2 mol. % illustrated more pronounced HA formation and better bioactivity than Ag-substituted BGs with 4 and 6 (mol. %) after immersion in SBF solution. Also, it was reported that spherical HA was formed on Ag-incorporated 58S BG, and by increasing immersion time up to 14 days, the amount of HA was enhanced [69]. Furthermore, Vulpoi et al. [59] reported that the bioactivity and biocompatibility of Ti/Ag-substituted BGs increased by increasing the percentage of Ag from 0 to 10 (mol. %). Hence, according to previous research, the presence of Ag with the different amounts in various types of BG had the same effect on bioactivity, and BG containing low amount of Ag between (1-3 mol. %) exhibited better HA formation on BG surface, and also, this investigation was in good agreement with related studies in the effect of Ag on BG overtime. Taken together, based on SEM results, TA2 BG had the best HA formation ability compared to all of the synthesized T/A-BGs.

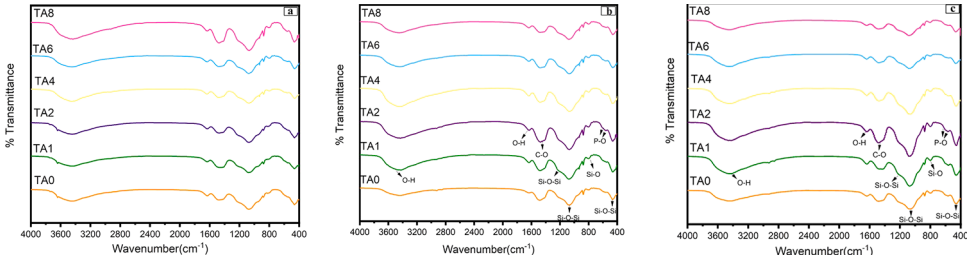


**Fig. 3.** The FTIR spectroscopy of T/A-BGs before immersion (a) and after immersion in the SBF solution for 7days (b) and 14 days(c).

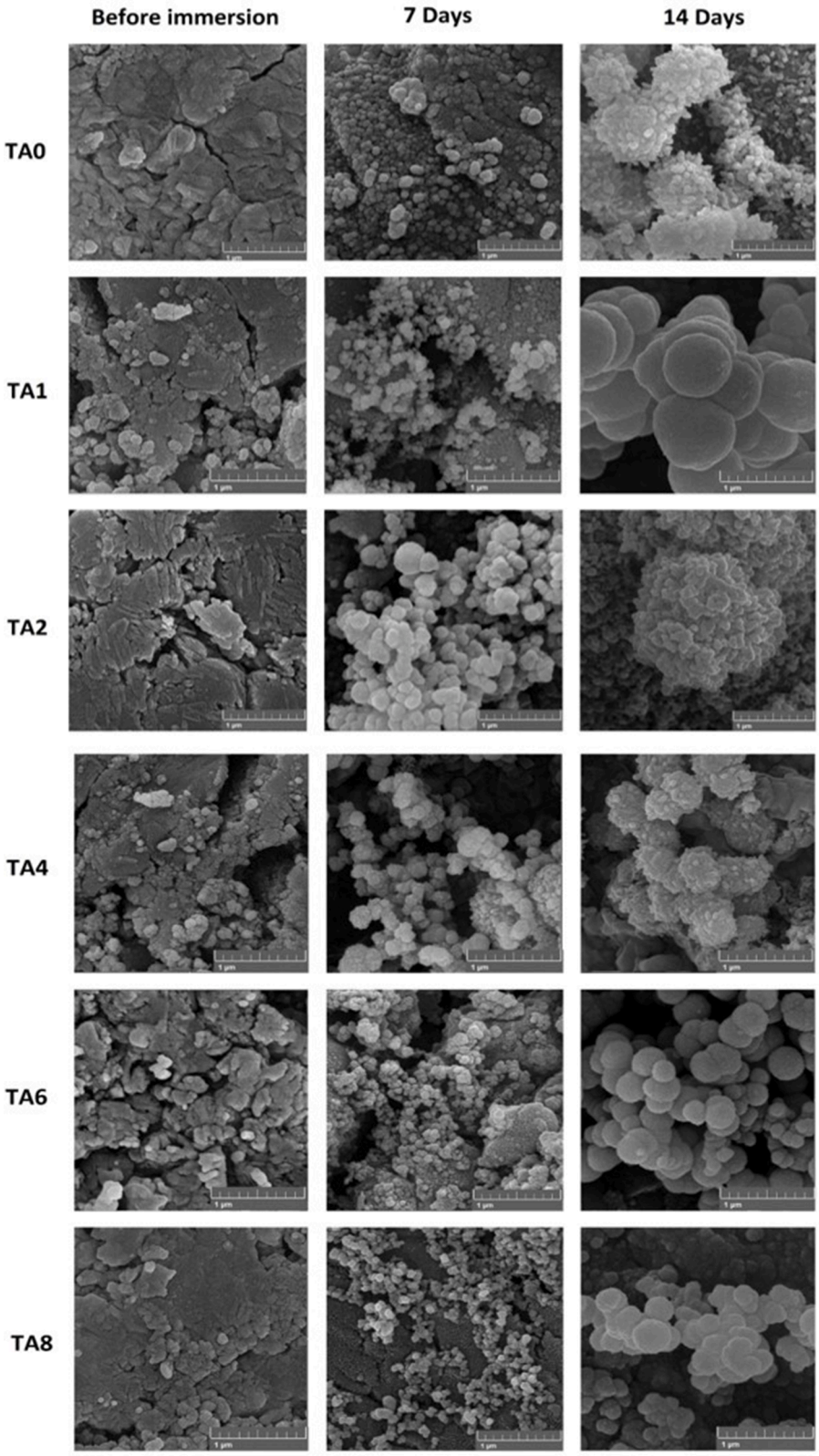


**Fig 4.** The SEM images of (a) TA0, TA1, and TA2, (b) TA4, TA6, and TA8 BGs before and after immersion in SBF solution for 7 and 14 days.

### *3.5. ICP analysis*

Fig. 6 illustrates the results of the ICP test on T/A-58S BGs that exhibited the function of Si, Ca, P, Ti, and Ag ions that release in SBF solution. The Ag ions released rapidly in the first three days of immersion and followed by, the release speed of Ag ions diminished by overtime up to 14 days. According to images, the concentration of Ag ions was in the range of 0-0.6 ppm. That means it was higher than the minimum value of bactericidal efficiency (0.1 ppm) and less than the maximum value for cytotoxicity of Ag (1.6 ppm) [70]. Additionally, the

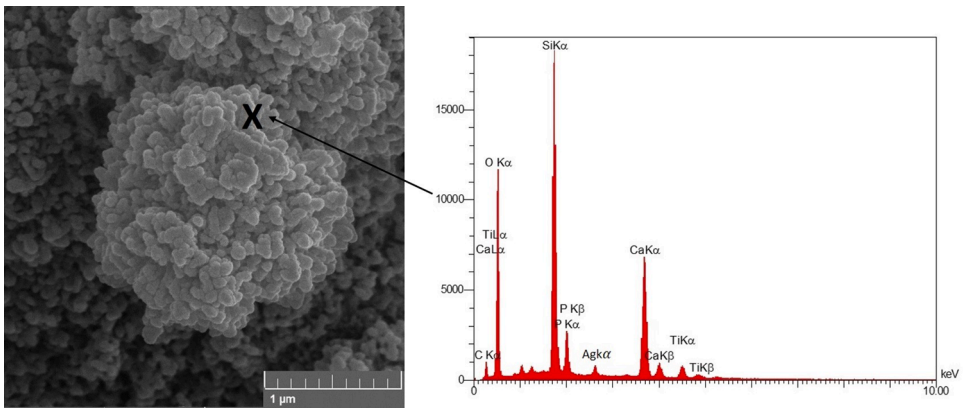


**Fig. 5.** The EDS spectroscopy of TA2 after immersion for 14 days in SBF solution.

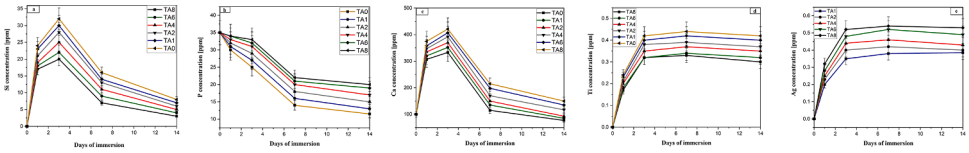

**Fig. 6.** The ions release rate of (a) Si, (b) Ca, (c) P, (d) Ti, and (e) Ag elements for 0,1, 3, 7, and 14 days.

Ca and Si concentration in SBF solution reduced by increasing immersion time after a sudden increase in Si and Ca ions releasing up to 3 days. In addition, the P ions concentration increased up to 3 days and after that, the ion release rate decreased due to the formation of HA. Besides, Jurczyk et al. [47] Confirmed the trend of altering P and Ca ions concentration by increasing immersion time. Furthermore, it was stated that [69] by increasing Ag amount substituted with CaO, Ag ions released rapidly in the first period of immersion time, which was followed by a decrease in its release rate in other days. Besides, Sharifianjazi et al. affirmed that [56] by increasing immersion time decreasing P concentration rate increased. Additionally, Simon. et al. reported that the high amount of Ti (8-10 mol. %) retarded the formation of HA but releases more Ag ions [71]. Hence, the trend of changing ions release rate was similar with previous studies, however, the different amount of ions release can be attributed to the various BG with varying methods of synthesis. Taken together, even though TA8 showed its excellence in ions release amount in comparison to other T/A-BGs but it could cause toxicity for BG.

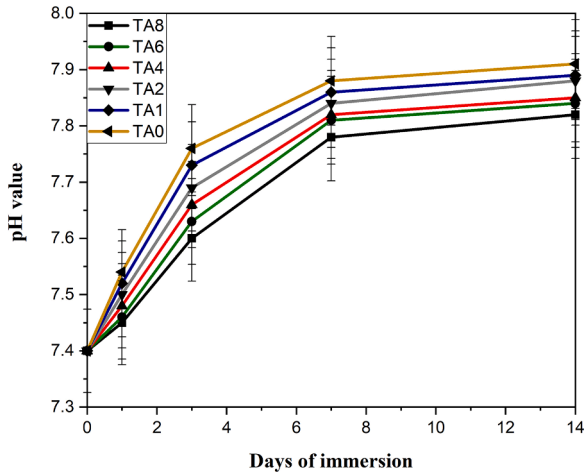


**Fig. 7.** The pH values of synthesized T/A-BGs for 0, 1, 3, 7, and 14 days.

### 3.6. pH values

pH value test was done on the SBF solution that TA-BGs were kept in it for different immersion time. As it is obvious, the results are exhibited in Fig. 7 and demonstrate that by increasing Ag percentage, the pH value decreased, but increasing immersion time had a different effect on pH value and led to increasing it. Additionally, pH value affected on bactericidal efficiency of TA2 and caused it to show more antibacterial activity in comparison to other T/A specimens. Moreover, Sharifianjazi et al. [56] reported that the range of pH value of sol-gel derived Ag-doped 58S BG was between 7.2 and 8.5, and also pH amount of BG containing 2 mol. % Ag was higher than BG, containing 4 and 6 (mol. %) after 3 days immersion. Besides, Nezafati et al. [72] affirmed that bactericidal efficiency of sol-gel derived 68S BG containing 0.5, 1, and 2 mol % Ag attributed to pH value and 0.5 mol. % Ag-substituted BG exhibited the highest antibacterial efficiency due to its high pH value in comparison to other Ag-BG specimens. According to previous research and our investigation, the trend of decreasing pH value according to Ag concentration and increasing pH value according to immersion time was the same, but the range of pH value was different that related to BGs composition. Hence, the TA2 exhibited the highest pH value after TA1 in comparison to other T/A-BGs with a higher amount of Ag.

### 3.7. In vitro biological evaluation

#### 3.7.1. Live-dead assay

To determine the effect of fixed 5 mol. % Ti and various amount of Ag on cell viability in T/A BGs, the TA0, and TA2 were assayed for 7 and 14 days incubation, and the results are exhibited in Fig. 8 According to the results, stained cells are in two different colors that green cells showed the live cells whiles red cells displayed dead cells. Additionally, the dead cells are more in TA0 than TA2, and by increasing incubation time up to 14 days, the accumulation of the cells enhanced in both TA0 and TA2, but it was more significant in TA2. Furthermore, it was stated that [15] the influence of Ag in sol-gel derived 58S-BG specimens were obvious and also BG containing 2 mol. % Ag exhibited more numbers of live cells than BG containing 6 mol. % Ag. Besides, Newby et al. [73] confirmed that foam replicating derived 45S5 BG containing a low percentage of Ag had better and more effective results in the number of live cells than

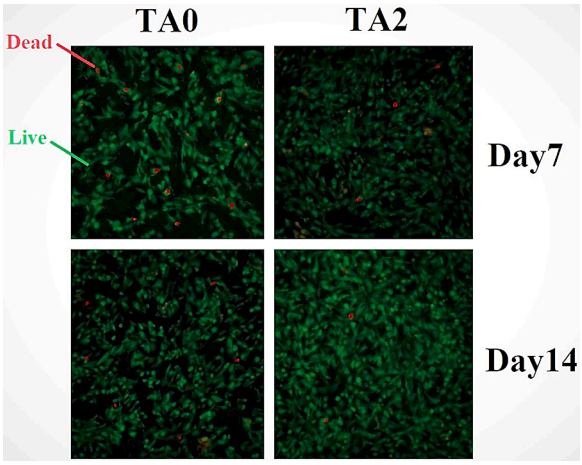


**Fig. 8.** The live (green)/ dead (red) fluorescence of MC3T3-E1 cells on TA0 and TA2 after 7 and 14 days. (For interpretation of the references ti color in this figure legend, the reader is referred to the the web version of this article.).

45S5 BG containing a high percentage of Ag. Hence, according to previous results and our investigation Ag had the same effect on the mentioned BG in live/dead assay. Besides, the presence of Ti and Ag together in all T/A-BGs caused that the specimens were not be toxic and were in good agreement with the MTT results (Fig. 9).

### 3.7.2. MTT assay

The stimulating effect of T/A-BGs on osteoblast-like cell line (MC3T3-E1) proliferation is described in Fig. 9 as it was revealed, in the 7 days of incubation, Firstly, an increase in cell proliferation of T/A-BGs was seen and then, by increasing Ag percentage more than 2 mol.%, OD decreased (*$p$<0.05). Furthermore, this trend was repeated in all incubation times, and the difference between TA2 and TA0 was significant in 14 days of immersion (**$p$<0.01). Additionally, by increasing immersion time up to 14 days, the cell proliferation improved in all T/A specimens. According to previous studies, Jurczyk et al. [43] reported that T/A-incorporated 45S5-BG displayed an increase in cell proliferation and an increase in the relative number of viable cells. Additionally, Phetnin et al. [74] reported that by increasing the percentage of Ag from 0 to 5 (mol. %) in Ag-incorporated 77S-BGs, cell viability percentage decreased. Moreover, Mariappan et al. [57] confirmed that for the Ag-substituted BG with 2 mol. %, not only a non-cytotoxic effect was detected on the osteoblastic cells of MC3T3.E1, but also had an acceleration effect on osteoblastic cells growth. Hence, according to the MTT results, it could be concluded that TA2 BG showed the highest MTT activity of MC3T3.E1 in comparison to other T/A-BGs.

### 3.7.3. ALP activity

The results of ALP activity on TA0, TA1, TA2, TA4, TA6, and TA8 were revealed after incubation for 0, 7, and 14 days. According to Fig. 10, it was evident that the ALP activity increased from 0 to 2 (mol. %) of Ag, and then, by increasing Ag percentage more than 2 mol. %, it decreased.

In other words, on the 7th day of immersion TA2 showed more ALP activity than BG with the lowest amount of Ag (TA0) and BG with the highest amount of Ag (TA8) in this study (*$p$<0.05). Additionally, this trend was similar in all incubation times, but it was more significant on the 14th day of immersion between TA2 and TA1 (**$p$<0.01). Furthermore, by increasing incubation time up to 14 days, the ALP activity of all T/A-BGs improved. Furthermore, it was confirmed that [51] Ag had an even effect on their BGs, and by increasing the Ag percentage to 4 mol. %, its effect increased, and then, by increasing Ag percentage more than 4 mol. % it decreased. Besides, Chernousova. et al. [75] affirmed that a high amount of Ag in sol-gel derived 45S5 BG led to cytotoxicity [38,76]. Hence, by increasing the incubation time up to 14 days, the ALP activity enhanced, and TA2 BG exhibited the highest ALP activity.

### 3.7.4. Antibacterial analysis

The antibacterial test was done on TA0, TA1, TA2, TA4, TA6, and TA8 and the results are shown in Fig. 11. According to the results, the effect of Ag as an antibacterial element is obvious on T/A-BGs. Additionally, the presence of Ti beside Ag enhanced the antibacterial efficiency in this assay. As it was evident, in the first 7 days of immersion, by increasing the amount of Ag up to 8 mol.%. Firstly, the antibacterial efficiency increased until to 2 mol. % Ag and then by increasing Ag percentage up to 8 mol. %, it decreased (*p < 0.05). In addition, this trend was repeated on the 14th day of immersion and was significant between T/A specimens, especially between TA2 and TA0 (**$p$<0.01). According to previous results, it was affirmed [43] that addition of Ag to BG containing Ti increased the antibacterial efficiency. Besides, it was reported that Ti and Ag-incorporated 45S5 BG with 1.5 mol. % Ag exhibited the lower adhesion of S.aureus and significant antibacterial activity [43]. Furthermore, It was confirmed that 45S5-BG substituted with 10 Ti and Ag (mol. %) showed the highest antibacterial efficiency due to Ag ions surrounded the environment and destroyed the bacteria cell walls [47].

Up to now, the main reasons for the antibacterial activity of BGs have not been discovered yet, but some possibilities explain it. The first one of

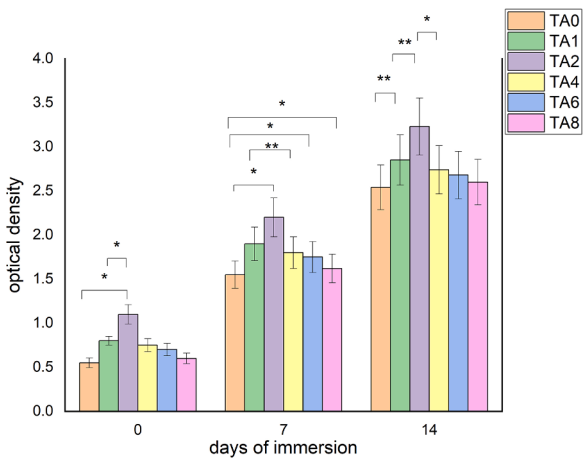


**Fig. 9.** The MTT activity of TA0, TA1, TA2, TA4, TA6, and TA8 after immersion for 0, 7, and 14 days (*$p$<0.05, **$p$<0.01).

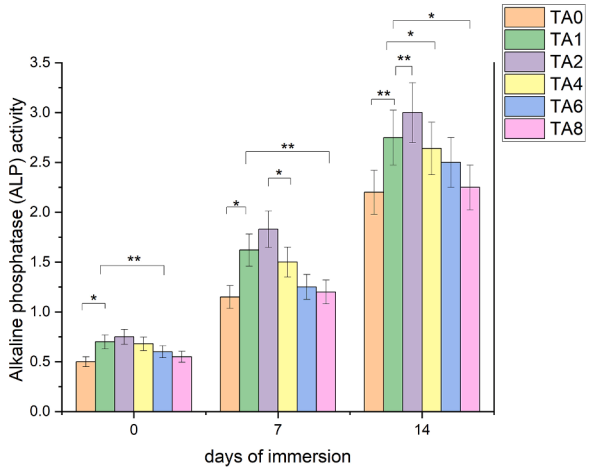


**Fig. 10.** The ALP activity of T/A-BG after immersion for 0, 7, and 14 days (*$p$<0.05, **$p$<" 0.01).

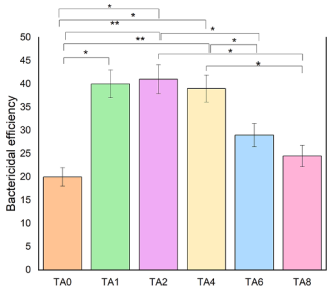


**Fig. 11.** The antibacterial efficiency of T/A-BG ("* $p<0.05$", "** $p<0.01$).

attributions was the release of alkaline earth ions, which caused an increase in pH values. Another reason was the release of ions such as calcium and phosphate that have a toxic effect on the bacteria [38,76]. Hence, T/A-BG exhibited high antibacterial efficiency because of their effects on pH values.

## 4. Conclusion

As a result, the 58S BG with formula 60 % $SiO_2$ – (36 – X) % CaO – 4% $P_2O_5$ – 5 % $TiO_2$ – X % $Ag_2O$, (X=0, 1, 2, 4, 6, and 8 mol. %) synthesized by sol-gel method and was investigated through some structural and biological analysis. According to the results, XRD patterns exhibited the HA peaks after immersion in SBF solution for 7 and 14 days. And by increasing the immersion time, the HA peaks were pronounced and confirmed that the HA formed increased. Additionally, the specimen with 5 Ti and 2 Ag (mol. %) (TA2) exhibited the highest bioactivity in comparison to all synthesized T/A-58S BGs. Besides, The FTIR images showed the Si, O, P, H, Ti, and Ag bonds and affirmed the formation of HA after immersion in SBF solution for 7 and 14 days. Furthermore, the different percentages of Ag altered the HA formed amount and TA2 exhibited the highest HA formation. The SEM images of T/A-BG revealed the globules of HA on the specimen surface. Also, by increasing immersion time, the bioactivity increased and the TA2 BG showed the highest bioactivity. Meanwhile, the EDS analysis detected the elements that were in the specimen. The biological assays such as MTT, ALP, and antibacterial activity exhibited the positive effect of Ag on cell proliferation, cell viability, and antibacterial efficiency. Moreover, ICP analysis and pH test determined the ions release and pH amount of elements, respectively. Taken together, TA2 BG was reported as the best candidate in providing cell viability, antibacterial, and *in vitro* bioactivity in comparison to others and could be considered as the optimal T/A-58S BG.

## Authors' contribution

All authors discussed the results and contributed to the final manuscript.

## CRediT authorship contribution statement

**Amirhossein Moghanian:** Investigation, Methodology, Supervision, Validation, Writing - original draft, Writing - review & editing. **Saba Nasiripour:** Investigation, Methodology, Validation, Writing - original draft. **Seyed Mohammad Hosseini:** Investigation, Methodology, Validation, Writing - original draft, Writing - review & editing. **Seyed Hesamedin Hosseini:** Investigation, Methodology, Visualization, Writing - original draft, Writing - review & editing. **Ali Rashvand:** Investigation, Methodology, Visualization, Writing - original draft. **Alireza Ghorbanoghli:** Investigation, Methodology, Visualization, Writing - original draft, Writing - review & editing. **Arang Pazhouheshgar:** Investigation, Methodology, Supervision, Writing - original draft. **Fariborz Sharifian Jazi:** Investigation, Methodology, Supervision, Writing - original draft, Writing - review & editing.

## Declaration of Competing Interest

The authors certify that they have NO affiliations with or involvement in any organization or entity with any financial interest (such as honoraria; educational grants; participation in speakers' bureaus; membership, employment, consultancies, stock ownership, or other equity interest; and expert testimony or patent-licensing arrangements), or non-financial interest (such as personal or professional relationships, affiliations, knowledge or beliefs) in the subject matter or materials discussed in this manuscript.

## References

[1] D. Khorsandi, A. Moghanian, R. Nazari, G. Arabzadeh, S. Borhani, Personalized medicine: regulation of genes in human skin ageing, J. Allergy Ther. 7 (2016) 2–11.
[2] A. Saatchi, A.R. Arani, A. Moghanian, M. Mozafari, Synthesis and characterization of electrospun cerium-doped bioactive glass/chitosan/polyethylene oxide composite scaffolds for tissue engineering applications, J. Ceram. Int. 47 (2020) 260–271.
[3] A. Moghanian, M. Zohourfazeli, Investigation the *in vitro* and bactericidal properties of magnesium and copper containing bioactive glasses, J. Adv. Mater. Technol. 9 (2020) 1–15. http://www.jamt.ir/article_117580_en.html.
[4] A. Moghanian, M. Mahdi Tajer, M. Zohourfazeli, Z. Miri, M. Saghafi Yazdi, Sol-gel derived silicate-based bioactive glass: studies of synergetic effect of zirconium and magnesium on structural and biological characteristics, J. Non-Cryst. Solids 554 (2020), 120613.
[5] A. Pazhouheshgar, S. Vanini, A. Moghanian, The experimental and numerical study of fracture behavior of 58s bioactive glass/polysulfone composite using the extended finite elements method, Mater. Res. Express 6 (2019), 095208. https://iopscience.iop.org/article/10.1088/2053-1591/ab3495/meta.
[6] A. Pazhouheshgar, A. Moghanian, S. Vanini, The extended finite element method numerical and experimental analysis of mechanical behavior of polysulfone/58s bioactive glass synthesized through solvent casting method, Modares Mech. Eng. 20 (2020) 2061–2073. https://mme.modares.ac.ir/article-15-37532-en.html.
[7] M. Tahriri, M. Del Monico, A. Moghanian, M. Yaraki, R. Torres, A. Yadegari, L. Tayebi, Graphene and its derivatives: opportunities and challenges in dentistry, Mater. Sci. Eng. C 102 (2019) 171–185.
[8] R. Clark, L. Hench, An investigation of bioactive glass powders by sol-gel processing, J. Appl. Biomateri. 2 (1991) 231–239.
[9] L. Hench, The story of Bioglass®, J. Mater. Sci. 17 (2006) 967–978.
[10] L. Hench, I. Thompson, Twenty-first century challenges for biomaterials, J. R. Soc. Interface 7 (2010) S379–S391.
[11] Y. Ikada, Challenges in tissue engineering, J of the Royal Society Interface 3 (2006) 589–601.
[12] A. Moghanian, M. Zohourfazeli, Comparative study on *in vitro*, physico-chemical and antibacterial properties of 58S and 68S bioactive glasses synthesized by sol-gel method, Adv. Process. Mater. 13 (2020) 17–30. https://www.sid.ir/en/Journal/ViewPaper.aspx?ID=716955.
[13] M. Cerruti, G. Magnacca, V. Bolis, C. Morterra, Characterization of sol–gel bioglasses with the use of simple model systems: a surface-chemistry approach, J. Mater. Chem. 13 (2003) 1279–1286.
[14] Z. Hajifathali, M. Amirhosseinian, The effect of substitution of CaO/MgO and CaO/SrO on *in vitro* bioactivity of sol-gel derived bioactive glass, Int. J. Biomed. Biol. Eng. 13 (2019) 279–287.
[15] A. Moghanian, M. Zohourfazeli, M. Mahdi Tajer, Z. Miri, S. Hosseini, A. Rashvand, Preparation, characterization and *in vitro* biological response of simultaneous co-substitution of $Zr^{+4}$/$Sr^{+2}$ 58S bioactive glass powder, Ceram. Int. (2020), https://doi.org/10.1016/j.ceramint.2020.11.139.
[16] M. Aminitabar, M. Amirhosseinian, M. Elsa, Synthesis and *in vitro* characterization of a gel-derived $SiO_2$-CaO-$P_2O_5$-SrO-$Li_2O$ bioactive glass, Int. J. Civ. Mech. Eng. 13 (2019) 296–307.
[17] A. Yao, D. Wang, Q. Fu, W. Huang, M. Rahaman, Preparation of bioactive glasses with controllable degradation behavior and their bioactive characterization, Chin. Sci. Bull. 52 (2007) 272–276.
[18] A. Moghanian, S. Firoozi, M. Tahriri, Characterization, *in vitro* bioactivity and biological studies of sol-gel synthesized SrO substituted 58S bioactive glass, J. Ceram. Int. 43 (2017) 14880–14890.
[19] A. Moghanian, F. Sharifianjazi, P. Abachi, E. Sadeghi, H. Jafarikhorami, A. Sedghi, Production and properties of Cu/$TiO_2$ nano-composites, J. Alloys Compd. 698 (2017) 518–524.
[20] N. Li, Q. Jie, S. Zhu, R. Wang, Preparation and characterization of macroporous sol–gel bioglass, J. Ceram. Int. 31 (2005) 641–646.
[21] P. Sepulveda, J.R. Jones, L. Hench, Characterization of melt-derived 45S5 and sol-gel–derived 58S bioactive glasses, J. Biomed. Mater. Res. 58 (2001) 734–740.
[22] P. Ehrl, J. Reuther, G. Frenkel, $Al_2O_3$-ceramic as material for dental implants, experimental and clinical study for the development of screw-and extension-implants, Int. J. Oral Surg. 10 (1981) 93–98.
[23] F. Shojaeepour, P. Abachi, K. Purazrang, A. Moghanian, Production and properties of Cu/$Cr_2O_3$ nano-composites, Powder Technol. 222 (2012) 80–84.

[24] A. Moghanian, A. Pazhouheshgar, A. Ghorbanoghli, Nonlinear viscoelastic modeling of synthesized silicate-based bioactive glass/polysulfone composite: theory and medical applications, Silicon (2020), https://doi.org/10.1007/s12633-020-00900-9.

[25] A. Pazhouheshgar, Y. Haghighatfar, A. Moghanian, Finite element method and analytical analysis of static and dynamic pull-in instability of a functionally graded microplate, J. Vib. Control (2020), https://doi.org/10.1177/1077546320980208.

[26] J. Li, B. Fartash, L. Hermansson, Hydroxyapatite—alumina composites and bone-bonding, Biomaterials 16 (1995) 417–422.

[27] M. Kazem-Rostami, A. Moghanian, Hünlich base derivatives as photo-responsive Λ-shaped hinges, Org. Chem. Front. 4 (2017) 224–228.

[28] A. Moghanian, R. Portillo-Lara, E. Shirzaei Sani, H. Konisky, S.H. Bassir, N. Annabi, Synthesis and characterization of osteoinductive visible light-activated adhesive composites with antimicrobial properties, J. Tissue Eng. Regen. Med. 14 (2020) 66–81.

[29] J. Ma, C. Chen, D. Wang, J. Hu, Synthesis, characterization and *in vitro* bioactivity of magnesium-doped sol–gel glass and glass-ceramics, J. Ceram. Int. 37 (2011) 1637–1644.

[30] M. Dziadek, B. Zagrajczuk, E. Menaszek, A. Wegrzynowicz, J. Pawlik, K. Cholewa-Kowalska, Gel-derived $SiO_2$–CaO–$P_2O_5$ bioactive glasses and glass-ceramics modified by SrO addition, J. Ceram. Int. 42 (2016) 5842–5857.

[31] C. Wu, Y. Zhou, M. Xu, P. Han, L. Chen, J. Chang, Y. Xiao, Copper-containing mesoporous bioactive glass scaffolds with multifunctional properties of angiogenesis capacity, osteostimulation and antibacterial activity, J. Biomater. 34 (2013) 422–433.

[32] A. El-Kady, A. Ali, Fabrication and characterization of ZnO modified bioactive glass nanoparticles, J. Ceram. Int. 38 (2012) 1195–1204.

[33] A. Moghanian, S. Firoozi, M. Tahriri, Synthesis and *in vitro* studies of sol-gel derived lithium substituted 58S bioactive glass, Ceram. Int. 43 (2017) 12835–12843.

[34] M.U Jurczyk, K. Jurczyk, A. Miklaszewski, M. Jurczyk, Design, nanostructured titanium-45S5 bioglass scaffold composites for medical applications, J of Materials & Design. 32 (2011) 4882–4889.

[35] A. El-Kady, A. Ali, R. Rizk, M. Ahmed, Synthesis, characterization and microbiological response of silver doped bioactive glass nanoparticles, Ceram. Int. 38 (2012) 177–188.

[36] K.T. Kim, M.Y. Eo, T.T.H. Nguyen, S.M. Kim, General review of titanium toxicity, International Journal of Implant Dentistry 5 (2019) 1–12.

[37] H. Chouirfa, H. Bouloussa, V. Migonney, C. Falentin-Daudré, Review of titanium surface modification techniques and coatings for antibacterial applications, J of Acta Biomaterialia 83 (2019) 37–54.

[38] S. Hu, J. Chang, M. Liu, C. Ning, Study on antibacterial effect of 45S5 Bioglass®, J. Mater. Sci. 20 (2009) 281–286.

[39] L. Ovington, The truth about silver, in: Ostomy/Wound management, 2004, 1S-10Sxv 50.9A Supp.

[40] C. Baker, A. Pradhan, L. Pakstis, D. Pochan, j. Darrin, S. Shah, Nanotechnology synthesis and antibacterial properties of silver nanoparticles, J of nanoscience and nanotechnology. 5.2 (2005) 244–249.

[41] A. Saatchi, A.R. Arani, A. Moghanian, M. Mozafari, Cerium-doped bioactive glass-loaded chitosan/polyethylene oxide nanofiber with elevated antibacterial properties as a potential wound dressing, Ceram. Int. (2020), https://doi.org/10.1016/j.ceramint.2020.12.078.

[42] K. Chaloupka, Y. Malam, A. Seifalian, Nanosilver as a new generation of nanoproduct in biomedical applications, Trends Biotechnol. 28 (2010) 580–588.

[43] K. Jurczyk, A. Miklaszewski, K. Niespodziana, M. Kubicka, M.U Jurczyk, M. Jurczyk, Synthesis and properties of Ag-doped titanium-10 wt% 45S5 bioglass nanostructured scaffolds, Journal of Acta Metallurgica Sinica (English Letters) 28 (2015) 467–476.

[44] M. Enright, D. Robinson, G. Randle, E. Feil, H. Grundmann, B. Spratt, The evolutionary history of methicillin-resistant *Staphylococcus aureus* (MRSA), Proc. Natl. Acad. Sci. 99 (11) (2002) 7687–7692.

[45] B. Ben-Arfa, I. Salvado, J. Ferreira, R. Pullar, The effect of functional ions ($Y^{3+}$, $F^{-}$, $Ti^{4+}$) on the structure, sintering and crystallization of diopside-calcium pyrophosphate bioglasses, J. Non-Cryst. Solids 443 (2016) 162–171.

[46] N. Vitko, A. Richardson, Laboratory maintenance of methicillin-resistant *Staphylococcus aureus* (MRSA), Curr. Protoc. Microbiol. 28 (2013), 9C. 2.1-9C. 2.14.

[47] K. Jurczyk, G. Adamek, M. Kubicka, J. Jakubowicz, M. Jurczyk, Nanostructured titanium-10 wt% 45S5 bioglass-Ag composite foams for medical applications, Materials 8 (2015) 1398–1412.

[48] S. Peng, P. Feng, P. Wu, W. Huang, Y. Yang, W. Guo, C. Gao, C. Shuai, Graphene oxide as an interface phase between polyetheretherketone and hydroxyapatite for tissue engineering scaffolds, Sci. Rep. 7 (2017) 1–14.

[49] J. Lee, H. Jang, K. Lee, H.-R. Baek, K. Jin, K. Hong, J. Noh, H.-K. Lee, In vitro and in vivo evaluation of the bioactivity of hydroxyapatite-coated polyetheretherketone biocomposites created by cold spray technology, Acta Biomater. 9 (2013) 6177–6187.

[50] T. Kokubo, Bioactive glass ceramics: properties and applications, Biomaterials 12 (1991) 155–163.

[51] A. Moghanian, M. Zohourfazeli, M.H.M Tajer, The effect of zirconium content on in vitro bioactivity, biological behavior and antibacterial activity of sol-gel derived 58S bioactive glass, J. Non-Cryst. Solids 546 (2020), 120262, https://doi.org/10.1016/j.jnoncrysol.2020.120262.

[52] C. Yellowley, Z. Li, Z. Zhou, C. Jacobs, H. Donahue, Functional gap junctions between osteocytic and osteoblastic cells, J. Bone Miner. Res. 15 (2000) 209–217.

[53] A. Moghanian, A. Ghorbanoghli, M. Kazem-Rostami, A. Pazhouheshgar, E. Salari, M. Saghafi Yazdi, T. Alimardani, H. Jahani, F. Sharifian Jazi, M. Tahriri, Novel antibacterial Cu/Mg-substituted 58S-bioglass: synthesis, characterization and investigation of in vitro bioactivity, Int. J. Appl. Glass Sci. 11 (2019) 685–698.

[54] S. Hu, C. Ning, Y. Zhou, L. Chen, K. Lin, J. Chang, Antibacterial activity of silicate bioceramics, J. Wuhan Univ. Technol.-Mater. Sci. Ed. 26 (2011) 226–230.

[55] A. Moghanian, A. Sedghi, A. Ghorbanoghli, E. Salari, The effect of magnesium content on in vitro bioactivity, biological behavior and antibacterial activity of sol–gel derived 58S bioactive glass, Ceram. Int. 44 (2018) 9422–9432.

[56] F. Sharifianjazi, N. Parvin, M. Tahriri, Synthesis and characteristics of sol-gel bioactive $SiO_2$-$P_2O_5$-CaO-$Ag_2O$ glasses, J. Non-Cryst. Solids 476 (2017) 108–113.

[57] C. Mariappan, N. Ranga, Influence of silver on the structure, dielectric and antibacterial effect of silver doped bioglass-ceramic nanoparticles, Ceram. Int. 43 (2017) 2196–2201.

[58] S. Heidari, T. Hooshmand, B. Yekta, A. Tarlani, N. Noshiri, M. Tahriri, Effect of addition of titanium on structural, mechanical and biological properties of 45S5 glass-ceramic, Ceram. Int. 44 (2018) 11682–11692.

[59] A. Vulpoi, L. Baia, S. Simon, V. Simon, E. C, Silver effect on the structure of $SiO_2$-CaO-$P_2O_5$ ternary system, Mater. Sci. Eng. :C. 32 (2012) 178–183.

[60] Z. Zhong, J. Qin, J. Ma, Electrophoretic deposition of biomimetic zinc substituted hydroxyapatite coatings with chitosan and carbon nanotubes on titanium, Ceram. Int. 41 (2015) 8878–8884.

[61] J. Ma, C. Chen, D. Wang, X. Meng, J. Shi, Influence of the sintering temperature on the structural feature and bioactivity of sol–gel derived $SiO_2$–CaO–$P_2O_5$ bioglass, Ceram. Int. 36 (2010) 1911–1916.

[62] X. Wu, G. Meng, S. Wang, F. Wu, W. Huang, Z. Gu, E. C, Zn and Sr incorporated 64S bioglasses: material characterization, *in-vitro* bioactivity and mesenchymal stem cell responses, Mater. Sci. Eng. :C. 52 (2015) 242–250.

[63] X. Zhang, Y. Wu, S. He, D. Yang, C. Technology, Structural characterization of sol–gel composites using TEOS/MEMO as precursors, Surf. Coat. Technol. 201 (12) (2007) 6051–6058.

[64] M. Elsa, A. Moghanian, Comparative study of calcium content on *in vitro* biological and antibacterial properties of silicon-based bioglass, Int. J. Civ. Mech. Eng. 13 (2019) 288–295.

[65] A. Moghanian, S. Firoozi, M. Tahriri, A. Sedghi, A comparative study on the *in vitro* formation of hydroxyapatite, cytotoxicity and antibacterial activity of 58S bioactive glass substituted by Li and Sr, Mater. Sci. Eng. C 91 (2018) 349–360.

[66] J. Moura, L. Teixeira, C. Ravagnani, O. Peitl, E.D. Zanotto, M. Beloti, H. Panzeri, A. Rosa, P. de Oliveira, *In vitro* osteogenesis on a highly bioactive glass-ceramic. (Biosilicate®), J. Biomed. Mater. Res. 82 (2007) 545–557.

[67] M. Mozafari, F. Moztarzadeh, M. Tahriri, Investigation of the physico-chemical reactivity of a mesoporous bioactive $SiO_2$–CaO–$P_2O_5$ glass in simulated body fluid, J. Non-Cryst. Solids 356 (2010) 1470–1478.

[68] J. da Silva Buriti, M. Barreto, F. Barbosa, B. de Brito Buriti, J. de Lima Souza, H. de Vasconcelos Pina, P. de Luna Rodrigues, M. Fook, Synthesis and characterization of Ag-doped 45S5 bioglass and chitosan/45S5-Ag biocomposites for biomedical applications, J. Therm. Anal. Calorim. (2020) 1–12, https://doi.org/10.1007/s10973-020-09734-4).

[69] M. Zohourfazeli, M. Mahdi Tajer, A. Moghanian, Comprehensive investigation on multifunctional properties of zirconium and silver co-substituted 58S bioactive glass, Ceram. Int. 47 (2021) 2499–2507.

[70] Y. Yan, X. Zhang, Y. Huang, Q. Ding, X. Pang, Antibacterial and bioactivity of silver substituted hydroxyapatite/$TiO_2$ nanotube composite coatings on titanium, Appl. Surf. Sci. 314 (2014) 348–357.

[71] V. Simon, C. Albon, S. Simon, Silver release from hydroxyapatite self-assembling calcium–phosphate glasses, J. Non-Cryst. Solids 354 (2008) 1751–1755.

[72] N. Nezafati, F. Moztarzadeh, S. Hesaraki, Surface reactivity and *in vitro* biological evaluation of sol gel derived silver/calcium silicophosphate bioactive glass, Biotechnol. Bioprocess Eng. 17 (2012) 746–754.

[73] P.J. Newby, R. El-Gendy, J. Kirkham, X.B. Yang, I.D. Thompson, A.R. Boccaccini, Ag-doped 45S5 Bioglass®-based bone scaffolds by molten salt ion exchange: processing and characterisation, Journal of Materials Science: Materials in Medicine 22 (3) (2011) 557–569.

[74] R. Phetnin, S. Rattanachan, Preparation and antibacterial property on silver incorporated mesoporous bioactive glass microspheres, J. Sol-Gel Sci. Technol. 75 (2015) 279–290.

[75] S. Chernousova, M. Epple, Silver as antibacterial agent: ion, nanoparticle, and metal, Angew. Chem. Int. Ed. 52 (2013) 1636–1653.

[76] I. Allan, H. Newman, M. Wilson, Antibacterial activity of particulate Bioglass® against supra-and subgingival bacteria, Biomaterials 22.1 (2001) 1683–1687.